http://www.jmaterenvironsci.com/

5-chloro-1-octylindoline-2,3-dione as a new corrosion inhibitor for mild steel in hydrochloric acid solution

Z. Tribak[1], Y. Kandri Rodi[1], H. Elmsellem[2*], I. Abdel-Rahman[3], A. Haoudi[1], M. K. Skalli[1], Y. Kadmi[4,5,6,7], B. Hammouti[2], M. Ali Shariati[8], E. M. Essassi[9,10]

[1]*Laboratoire de chimie appliquée/organique appliquée. Faculté des Sciences et Techniques, Université Sidi Mohamed Ben Abdallah, BP 2202 Fès, Morocco.*

[2]*Laboratoire de chimie analytique appliquée, matériaux et environnement (LC2AME), Faculté des Sciences, B.P. 717, 60000 Oujda, Morocco.*

[3]*Department of Chemistry, College of Sciences, University of Sharjah, PO Box: 27272, UAE.*

[4]*Université d'Artois, EA 7394, Institut Charles Viollette, Lens, F-62300, France*

[5]*ISA Lille, EA 7394, Institut Charles Viollette, Lille, F-59000, France*

[6]*Ulco, EA 7394, Institut Charles Viollette, Boulogne sur Mer, F-62200, France*

[7]*Université de Lille, EA 7394, Institut Charles Viollette, Lille, F-59000, France*

[8]*Research Department, LLC «Science & Education», and Researcher, All Russian Research Institute of Phytopathology, Moscow Region, Russia.*

[9]*Laboratoire de Chimie Organique Hétérocyclique, URAC 21, Pôle de Compétences Pharmacochimie, Mohammed V University in Rabat, Faculté des Sciences, Av. Ibn Battouta, BP 1014 Rabat, Morocco.*

[10]*Moroccan Foundation for Advanced Science, Innovation and Research (MASCIR), Rabat Design Center, Rue Mohamed Al Jazouli, Madinat El Irfane, Rabat, Morocco.*

Abstract

In this study 5-chloro-1-octylindoline-2,3-dione (E1) was synthesized, characterized and tested as a new corrosion inhibitor for mild steel in 1M HCl solution. Weight-loss and potentiodynamic polarization measurements were applied to analyse the metal corrosion behaviour in the absence and presence of different concentrations of the inhibitor E1. The results obtained revealed that this compound has fairly good inhibiting properties for mild steel corrosion in 1M HCl solution, with efficiency of around 90 % at a concentration of 10^{-3}M. The inhibition was of a mixed anodic–cathodic nature. The adsorption of the inhibitor on the surface of mild steel was found to obey Langmuir adsorption isotherm. SEM study showed the formation of a protective adsorptive film of the inhibitor on mild steel surface.

1. Introduction

In the industrial field, acidic media such as sulfuric and hydrochloric acids are applied to remove undesirable substances or corrosion products from metallic materials [1]. However, metal corrosion occurs during deterioration of metals or alloys by the electrochemical reaction accompanied by various influences. Worldwide severe economic losses are caused by this corrosion in industrial areas [2].

In order to prevent corrosion and reduce the use of acid, organic corrosion inhibitors present in the system, most of its inhibitors contain nitrogen, sulfur and oxygen atoms [3-6]. In particular, an electrostatic interaction will occur between the metal surface and the inhibitory molecules, through these heteroatoms contained in the structure of the inhibitor [7], which will further prevent the target surface from interacting directly with the erosive materials. As a result, the corrosion rate will be reduced, which will extend the life of the target. Certain organic inhibitors containing nitrogen-based groups have been developed and have shown an intriguing

corrosion inhibiting performance. The inhibiting mechanism is generally explained by the formation of a physically and/or chemically adsorbed film on the metal surface [8, 9]. View the extended applications of isatin derivatives in various fields of biology, medicine, industry and because of their anti-fungal [10], antibacterial [11], anticonvulsant [12], anti HIV [13], antidepressant [14], anti-inflammatory [15] and anticorrosive properties [16], we have synthesized a new heterocyclic compound derived from 5-Chloroisatin as new corrosion inhibitor in acidic media.

In this work, the efficacy of the organic compound 5-chloro-1-octylindoline-2,3-dione (**Figure 1**) as corrosion inhibitor of mild steel is reported using weight loss, electrochemical impedance spectroscopy (EIS), Tafel polarization methods and quantum chemical calculations.
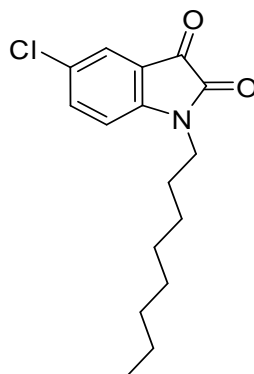

Figure 1. Chemical structure of 5-chloro-1-octylindoline-2,3-dione (E1).

2. Experimental

2.1. Synthesis of inhibitor

To a solution of 5-chloroisatin (0,4 g, 2,20 mmol) in N-N-dimethylformamide (15 ml), was added potassium carbonate (0.23g, 1.16 mmol) and (0.035g, 0.10mmol) tetra n-butylammonium bromide (TBAB) (0.035g, 0.10mmol), after that the brominated reagent was added slowly. The reaction mixture was stirred for 48 hours at room temperature. After the filtration and treatment of the reaction, the solution was evaporated under reduced pressure. The residue obtained was recrystallized from ethanol to afford red crystals with good yield.
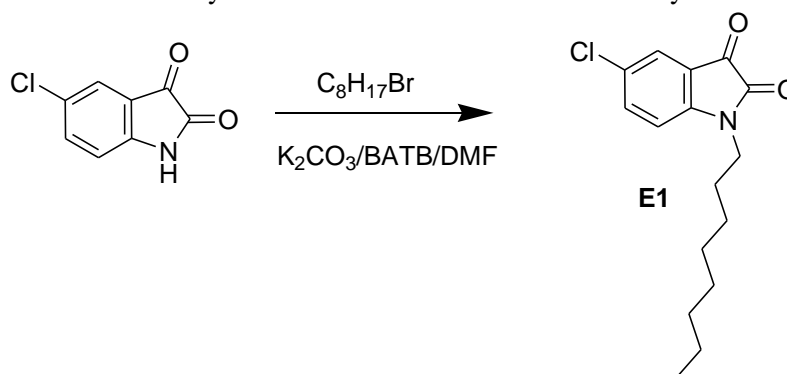
Scheme 1. Synthesis of 5-chloro-1-octylindoline-2,3-dione (E1).

Yield: 88% ; mp: 341K ; ^{1}H NMR **(CDCl$_3$; 300MHz) δ (ppm) :** 7.54-7.55(d, H, H$_{Ar}$, ^{4}J$_{H-H}$ =3Hz) ; 7.50-7.51(d, H, H$_{Ar}$, ^{4}J$_{H-H}$ =3Hz) ; 6.84(d, H, H$_{Ar}$, ^{3}J$_{H-H}$ =9Hz) ; 3.68(t, 2H, CH$_2$, ^{3}J$_{H-H}$ = 6Hz) ; 1.71-1.53(m, 2H, CH$_2$) ; 1.24-1.31(m, 10H,CH$_2$), 0.85(t, 3H, CH$_3$, ^{3}J$_{H-H}$ =6Hz). ^{13}**C NMR (CDCl$_3$;75MHz) δ(ppm) :** 183.20(C=O) ; 160.73(N-C=O); 144.60, 137.60, 125.37(Cq); 129.45, 115.79, 111.42 (CH$_{Ar}$); 40.47, 31.73, 29.19, 27.20, 26.88, 22.60(CH$_2$) ; 14.04(CH$_3$).

2.2. Metal specimen

Corrosion tests were performed on a mild steel of the following percentage composition (weight per cent): 0.21C, 0.38Si, 0.09P, 0.05Mn, 0.05S, 0.01Al and the remainder iron.

2.3. Aggressive solution

The aggressive solution used was made of AR grade 37 % HCl. A 1M solution of the acid was prepared using bidistilled water. The concentration range of the inhibitor employed was 10^{-6} M to 10^{-3} M, in 1M HCl.

2.4. Weight loss measurements

Gravimetric measurements were carried out in double walled glass cell equipped with a thermostatic cooling condenser. The solution volume was 100 cm3, the temperature was 308 ± 1 K and the immersion time was 6 h. Each experiment was repeated at least three times to ensure reproducibility and average weight loss was noted. The inhibition efficiency (%) was determined by following equation:

$$Ew \% = \frac{V_0 - V}{V_0} X\ 100 \quad (1)$$

Where: v_0 and v are, respectively, the values of corrosion rate with and without inhibitor.

2.4.1. Electrochemical Measurements

The electrochemical measurements were carried out using Volta lab (Tacussel - Radiometer PGZ 100) potentiostat controlled by Tacussel corrosion analysis software model (Voltamaster 4) at static condition. The corrosion cell used had three electrodes. The reference electrode was a saturated calomel electrode (SCE). A platinum electrode was used as auxiliary electrode of surface area of 1 cm^2. The working electrode was carbon steel of the surface 1cm^2. All potentials given in this study were referred to this reference electrode. The working electrode was immersed in the test solution for 30 minutes to establish a steady state open circuit potential (E_{ocp}). After measuring the E_{ocp}, the electrochemical measurements were performed. All electrochemical tests have been performed in aerated solutions at 308 K. The EIS experiments were conducted in the frequency range with high limit of 100 kHz and different low limit 0.1 Hz at open circuit potential, with 10 points per decade, at the rest potential, after 30 min of acid immersion, by applying 10 mV ac voltage peak-to-peak. Nyquist plots were made from these experiments. The best semicircle can be fit through the data points in the Nyquist plot using a non-linear least square fit so as to give the intersections with the x-axis.

2.5. Quantum Chemical Calculations

All the quantum chemical calculations have been carried out with Gaussian 09 programme package [17-18]. In our calculation we have used B3LYP, a hybrid functional of the DFT method, which consists of the Becke's three parameters; exact exchange functional B3 combined with the nonlocal gradient corrected correlation functional of Lee-Yang-Par (LYP) has been used along with 6-31G(d, p) basis set. In the process of geometry optimisation for the fully relaxed method, convergence of all the calculations has been conirmed by the absence of imaginary frequencies. The aim of our calculation is to calculate the following quantum chemical indices: the energy of highest occupied molecular orbital (E_{HOMO}), the energy of lowest unoccupied molecular orbital (E_{LUMO}), energy gap (ΔE), hardness (η), sotness (σ), electrophilicity index (ω), the fraction of electrons transferred (ΔN) from inhibitor molecule to the metal surface, and energy change when both processes occur, namely, and correlate these with the experimental observations.

The electronic populations as well as the Fukui indices and local nucleophilicities are computed using NPA (natural population analysis) [19–21]. Our objective, in this study, is to investigate computationally inhibitory action of isatin derivative **E1** with chloridric acid in gas and in aqueous phase using B3LYP method with 6-31G(d, p) basis set.

2.5.1. Theory and computational details

Theoretical study of bezothiazine derivative with chloridric acid as corrosion inhibitors was done by using the Density Functional Theory (DFT) with the B3LYP [22] /6-31G(d, p) method implemented in Gaussian 09 program package.

In this study, some molecular properties were calculated such as the frontier molecular orbital (HOMO and LUMO) energies, energy gap (E_{Gap}), charge distribution, electron affinity (A), ionization

Popular qualitative chemical concepts such as electronegativity [23, 24] (χ) and hardness [25] (η) have been provided with rigorous definitions within the purview of conceptual density functional theory [26–28].

Using a finite difference method, working equations for the calculation of χ and η may be given as [26]:

$$\chi = \frac{I+A}{2} \quad or \quad \chi = -\frac{E_{HOMO}+E_{LUMO}}{2} \qquad (2)$$

$$\eta = \frac{I-A}{2} \quad or \quad \eta = -\frac{E_{HOMO}-E_{LUMO}}{2} \qquad (3)$$

Where I = -E_{HOMO} and A= -E_{LUMO} are the ionization potential and electron affinity respectively.

Local quantities such as Fukui function defined the reactivity/selectivity of a specific site in a molecule.

Using left and right derivatives with respect to the number of electrons, electrophilic and nucleophilic Fukui functions for a site k in a molecule can be defined [29].

$$f_k^+ = q_k(N+1) - q_k(N) \quad for\ nucleophilic\ attack \qquad (4)$$

$$f_k^- = q_k(N) - q_k(N-1) \quad for\ electrphilic\ attack \qquad (5)$$

$$f_k^+ = [q_k(N+1) - q_k(N-1)]/2 \quad for\ radical\ attack \quad (6)$$

where, $q_k(N)$, $q_k(N+1)$ and $q_k(N-1)$ are the natural populations for the atom k in the neutral, anionic and cationic species respectively.

The fraction of transferred electrons ΔN was calculated according to Pearson theory [30]. This parameter evaluates the electronic flow in a reaction of two systems with different electronegativities, in particular case; a metallic surface (Fe) and an inhibitor molecule. ΔN is given as follows:

$$\Delta N = \frac{\chi_{Fe} - \chi_{inh}}{2(\eta_{Fe} + \eta_{inh})} \qquad (7)$$

where χ_{Fe} and χ_{inh} denote the absolute electronegativity of an iron atom (Fe) and the inhibitor molecule, respectively; η_{Fe} and η_{inh} denote the absolute hardness of Fe atom and the inhibitor molecule, respectively. In order to apply the eq. 7 in the present study, a theoretical value for the electronegativity of bulk iron was used χ_{Fe} = 7 eV and a global hardness of η_{Fe} = 0, by assuming that for a metallic bulk I = A because they are softer than the neutral metallic atoms [30].

The electrophilicity has been introduced by Parr et al. [31], is a descriptor of reactivity that allows a quantitative classification of the global electrophilic nature of a compound within a relative scale. They have proposed the ω as a measure of energy lowering owing to maximal electron flow between donor and acceptor and ω is defined as follows.

$$\omega = \frac{\chi^2}{2\eta} \qquad (8)$$

The Softness σ is defined as the inverse of the η [32].

$$\sigma = \frac{1}{\eta} \qquad (9)$$

2.6. Surface morphology
Scanning electron microscopic study was employed to analyze the surface characteristics of the mild steel immersed in 1M HCl with and without the inhibitor E1. The morphology was recorded using CARL ZEISS (zigma 5, UK).

3. Results and discussion
3.1. Mass loss measurements
Mass loss of mild steel in mg/cm^2 was determined in the absence and presence of different concentrations (10^{-6} – 10^{-3} M) of the E1. The percentage inhibition efficiency, corrosion rate and surface coverage were calculated from the mass loss and are recorded in Table 1. In both the compounds the increase in inhibitor concentration results in a decrease in mass loss and an increase in percentage inhibition efficiency. Maximum of 90% was obtained with E1 at 10^{-3} M and was considered as the optimum concentration.

3.2. Surface coverage and adsorption isotherm
The coverage of E1 on mild steel active sites and formation of thin protective film that shields metal surface from the aggressive acid could have led to the reduction in corrosive attack.

Fractional surface coverage data were fitted into different adsorption isotherm models to help explain the nature of interaction in the adsorbed layer. The models tested were Langmuir, Temkin, Freundlich, Florry Hugins and Frumkin.

Table 1: Impedance parameters with corresponding inhibition efficiency for the corrosion of mild steel in 1.0 M HCl at different concentrations of (**E1**).

Inhibitor	Concentration (M)	v (mg.cm^{-2}h^{-1})	E_w (%)	θ
1M HCl	**--**	0.82	--	--
E1	**10^{-6}**	0.34	59	0.59
	10^{-5}	0.23	72	0.72
	10^{-4}	0.13	84	0.84
	10^{-3}	0.08	**90**	0.90

While the coverage data of E1 on the mild steel best fitted into Langmuir models ($R^2 \geq 0.998$). The plots in Figure 2 depict linear fittings obtained from Langmuir adsorption isotherm. The parameters deduced from the plot are listed in Table 2. The Langmuir isotherms can be expressed as shown in Eq. (10) below.

$$\frac{C}{\theta} = \frac{1}{k} + C \quad (10)$$

Table 2. Parameters deduced from Langmuir adsorption isotherm for E1.

Inhibitor	Slope	R^2	K_{ads} (M^{-1})	ΔG°_{ads} (kJ mol^{-1})
E1	1.10781	0.999	2.67E+05	-42.26
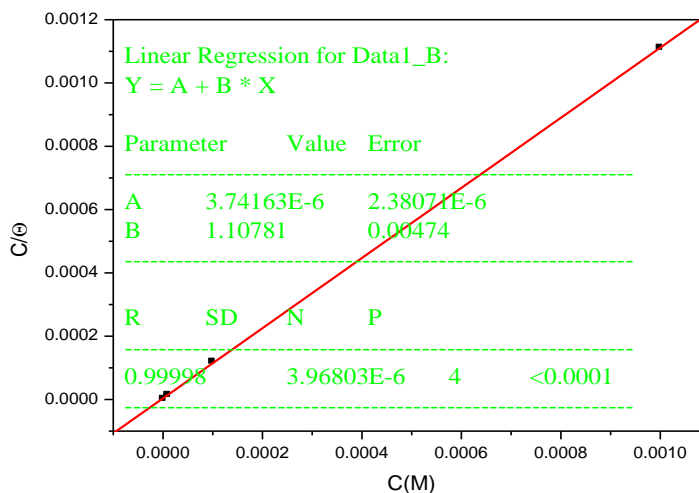
Figure 2. C/θ versus C plots for mild steel in 1 M HCl at 308K at the presence of (θ is mean values of surface coverage from potentiodynamic polarization measurements).

The free energy of adsorption (ΔG_{ads}) was calculated from K_{ads} values using Eq. (11).

$$\Delta G_{ads} = -RT \ln(55.5 K_{ads}) \quad (11)$$

where 55.5 represents the molar concentration of water. In literature, when values of ΔG_{ads} is around −20 kJmol^{-1}, the adsorption involves electrostatic interaction (physisorption) while ΔG_{ads} values above −40 kJmol^{-1} is attributed to chemisorption [33]. Most of the values obtained in this study are less than −20 kJmol^{-1} and can be attributed to physical adsorption mechanism. Results also show possibility of chemical adsorption occurring

on mild steel surface. Such observations can be also be found in literature [34]. The negative ΔG_{ads} values also indicate that the adsorption of E1 on the metal surfaces is spontaneous.

3.3. Potentiodynamic polarization measurements

Figure 3 shows the cathodic and anodic polarization curves of mild steel in 1M HCl solution without and with different concentrations of E1 at 308 K. Values of all electrochemical parameters such as corrosion potential (E_{corr}), cathodic and anodic Tafel slopes (βc, βa) and corrosion current density (I_{corr}) attained by extrapolation of Tafel lines, as well as inhibitor efficiency are listed in Table 3.

From Figure 3, it is clear that the values of (I_{corr}) of mild steel in the inhibited solution were smaller than those for the inhibitor-free solution. The addition of E1 induces a decrease in both cathodic and anodic currents. This result shows that the addition of E1 hindered the acid attack on the steel electrode.
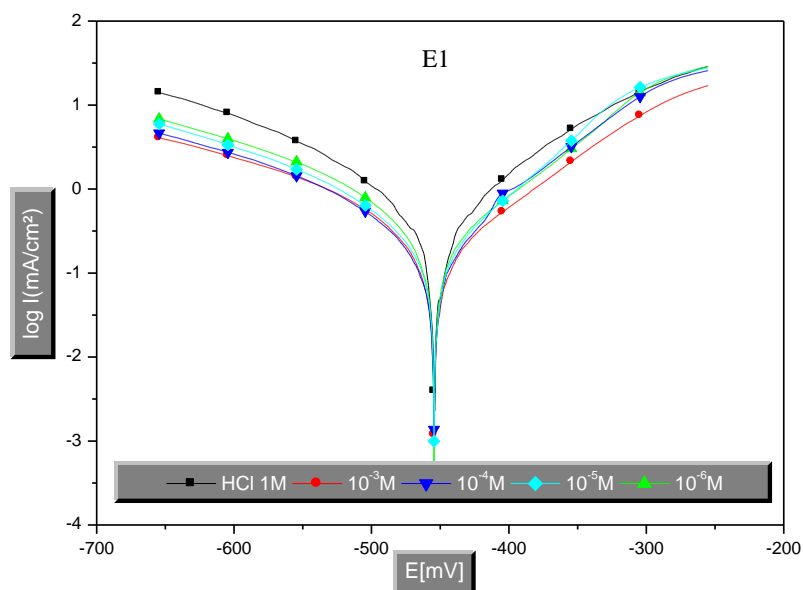
Figure 3. Polarization curves for mild steel in 1M HCl without and with different concentration of E1.

Table 3. Electrochemical parameters for mild steel in absence and presence of different concentrations of E1 at 308K obtained from Tafel extrapolation.

Inhibitor	Concentration (M)	$-E_{corr}$ (mV/SCE)	I_{corr} ($\mu A/cm^2$)	$-\beta_c$ (mV dec^{-1})	β_a (mV dec^{-1})	E_p (%)
1M HCl	**-**	465	1387	184	203	--
5-chloro-1-octylindoline-2,3-dione (E1)	**10^{-6}**	461	612	177	201	56
	10^{-5}	459	401	193	195	71
	10^{-4}	455	273	178	199	80
	10^{-3}	457	143	172	198	**90**

Further inspection of Figure 3 reveals that in the cathodic range, the cathodic currents densities were less sensitive to E1 concentration while in the anodic range, a significant decrease in the anodic current densities lead to a shift of the corrosion potentials (E_{corr}) toward more positive direction are noted when the inhibitor concentration increased. Therefore, it could be concluded that this compound can be classified as a mixed type inhibitor for mild steel in 1M HCl [35].

It is also noticed as can be seen from of Table 3 that the presence of different concentration of E1 did not change significantly the cathodic and anodic Tafel slope values (β_c , β_a) relative to the blank. This finding would indicate that the inhibition effect is caused by blocking of metal surface electrode by adsorbed inhibiting species without affecting the anodic and cathodic reaction mechanism[36-37].

3.4. Electrochemical impedance spectroscopy measurements

The experimental impedance results of mild steel in 1 M HCl with and without inhibitor are displayed in Figures 4 It is clear that the impedance response of mild steel is significantly changed after addition of 5-chloro-1-octylindoline-2,3-dione (E1) and the diameter of the semi-circle increases. The complex plane plot (Nyquist) obtained in the absence and presence of inhibitor shows one capacitive loop at high frequency region. The capacitive loop is attributed to the charge transfer resistance parallel to double-layer capacitance[38-39].

In order to determine the impedance parameters from the experimental results, the data were fitted to the electrical equivalent circuit using the Zview software. Figure 5 represents the electrical equivalent circuit in the absence and presence of inhibitor E1. Excellent fit results in Figure 6 (with 10^{-3}M E1) were obtained using this circuit. In the equivalent circuit, R_s is the uncompensated solution resistance, R_{ct} refers to the charge-transfer resistance and CPE is the constant phase element (CPE). The calculated impedance parameters derived from the complex plane plots are given in Table 4. In this case, due to the depression resulted by surface heterogeneity at a micro- or nano-level, such as the surface roughness/porosity, adsorption or diffusion, an acceptable fit could be obtained only if a CPE is used instead of capacitance in the equivalent circuit models [40-41].
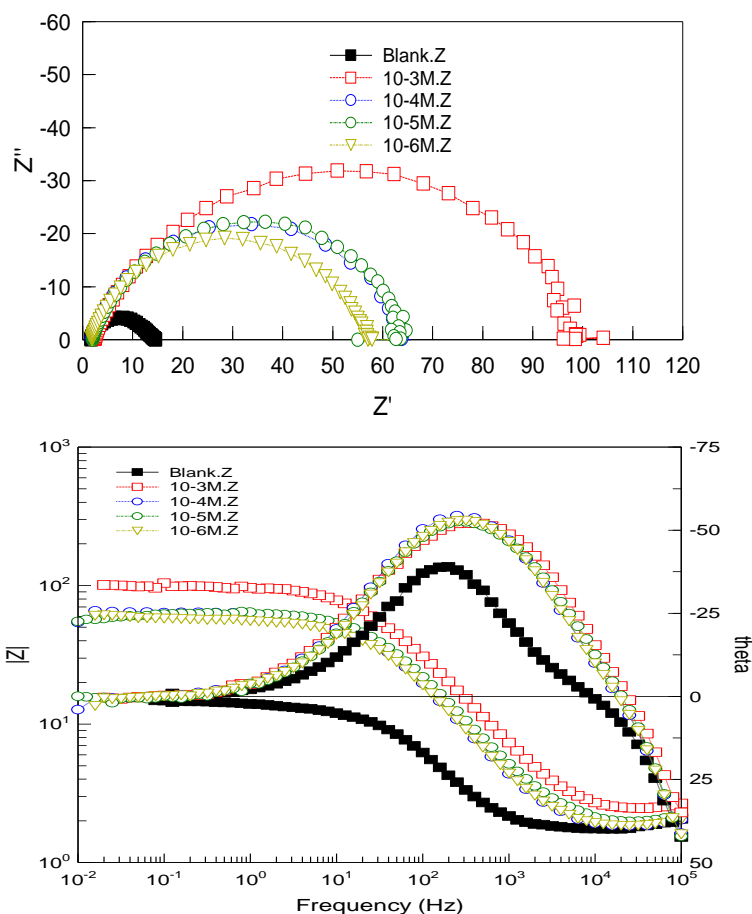

Figure 4. Electrochemical impedance plots of mild steel in 1 M HCl with 10^{-6}-10^{-3}M (by weight) of E1 at OCP and 308K: (a) Nyquist, (b) Bode-Z, and Bode-Phase plots (solid lines show fitted results).

As evident from Table 4, the values of charge-transfer resistance have increased with increasing the inhibitors concentration. This may be attributed to the decrease in local dielectric constant and/or to the increase in the thickness of the electrical double layer [42-43]. These results suggest that the 5-chloro-1-octylindoline-2,3-dione (E1) act just via adsorption at the metal/solution interface. The dissolution mechanism could be predicted by the values of phase shift (n) as an indicator. It is clear that, no significant change in the value of n is observed after addition of various concentrations of inhibitor E1 (Table 4). The almost invariable values of n indicates that the charge transfer process controls the dissolution mechanism in both the absence and presence of various concentrations of 5-chloro-1-octylindoline-2,3-dione (E1) [44-45]. The aforementioned results indicate that the EIS and potentiodynamic polarization measurements data correlate well with each other.

Table 4. EIS parameters obtained for mild steel in 1 M HCl in absence and presence of different concentration of E1 inhibitor.

Concentration (M) / Prameters	1M HCl	10^{-6}	10^{-5}	10^{-4}	10^{-3}
Real Center	9.25	29.782	32.104	32.621	50.959
Imag. Center	1.62	11.653	7.8581	10.131	20.468
Diameter	15.13	60.982	61.557	64.761	105.38
n	0.81	0.83	0.87	0.85	0.82
Low Intercept R_s ($\Omega.cm^2$)	1.86	1.6058	2.3458	1.8663	2.4094
High Intercept R_t ($\Omega.cm^2$)	16.64	57.958	61.862	63.376	99.509
Depression Angle	12.42	22.47	14.792	18.232	22.86
ω_{max} (rad s^{-1})	929.60	182.27	200.61	167.57	156.86
Estimated R_t ($\Omega.cm^2$)	14.78	52.35	57.51	65.51	97.09
Estimated C_{dl} (F.cm^{-2})	7.11 E-5	6.9968E-5	6.098E-5	5.215E-5	5.0498E-5
E (%)	--	72	74	77	**85**
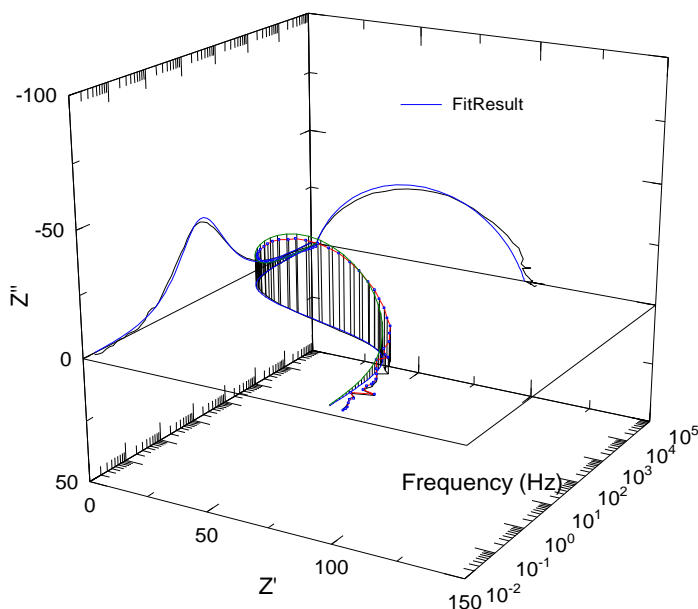
Figure 5. EIS Nyquist and Bode diagrams 3D for mild steel/1 M HCl + 10^{-3} M of E1 interface: (**------**) experimental; (**------**) fitted data.
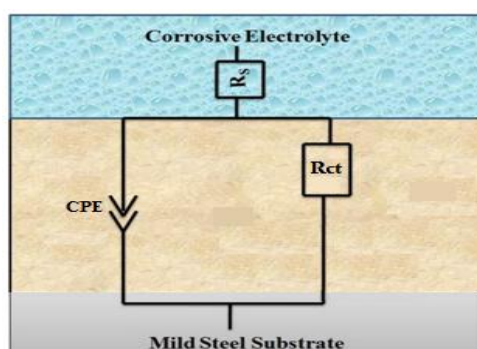
Figure 6. Equivalent circuit used to model metal/solution interface of mild steel in 1 M HCl in the absence and presence of inhibitors (for equivalent circuit diagram, Rs: uncompensated solution resistance, R$_{ct}$: charge-transfer resistance and CPE: constant phase element.

3.5. Quantum chemical calculations

In the last few years, the FMOs (HOMO and LUMO) are widely used for describing chemical reactivity. The HOMO containing electrons, represents the ability (EHOMO) to donate an electron, whereas, LUMO haven't not electrons, as an electron acceptor represents the ability (ELUMO) to obtain an electron. The energy gap between HOMO and LUMO determines the kinetic stability, chemical reactivity, optical polarizability and chemical hardness–softness of a compound [46].

In this paper, we calculated the HOMO and LUMO orbital energies by using B3LYP method with 6-31G(d,p). All other calculations were performed using the results with some assumptions. The higher values of E_{HOMO} indicate an increase for the electron donor and this means a better inhibitory activity with increasing adsorption of the inhibitor on a metal surface, whereas E_{LUMO} indicates the ability to accept electron of the molecule. The adsorption ability of the inhibitor to the metal surface increases with increasing of E_{HOMO} and decreasing of E_{LUMO}.

High ionization energy (I= 6.18 eV, I= 6.74 eV in gas and aqueous phases respectively) indicates high stability [47-48], the number of electrons transferred (ΔN) was also calculated and tabulated in Table 5. The number of electrons transferred (ΔN) was also calculated and tabulated in Table 6. The ΔN(gas) < 3.6 and ΔN(aqueous) < 3.6 indicates the tendency of a molecule to donate electrons to the metal surface [49-50].

Table 5. Quantum chemical descriptors of the studied inhibitor at B3LYP/6-31G(d, p) in gas, G and aqueous, A phases.

|	Phase	
Prameters	**Gas**	**Aqueous**
Total Energy *TE* (eV)	-35017.1	-35017.5
E_{HOMO} (eV)	-6.3709	-6.5165
E_{LUMO} (eV)	-2.8228	-3.1945
Gap *ΔE* (eV)	3.5480	3.3219
Dipole moment *μ* (Debye)	6.1043	8.0983
Ionisation potential *I* (eV)	6.3709	6.5165
Electron affinity *A*	2.8228	3.1945
Electronegativity *χ*	4.5968	4.8555
Hardness *η*	1.7740	1.6609
Electrophilicity index *ω*	5.9557	7.0971
Softness *σ*	0.5636	0.6020
Fractions of electron transferred *ΔN*	0.6773	0.6455

The calculated values of the f_k^+ for inhibitor are mostly localized on the isatin ring. Namely C_3, C_6, Cl_{12} and O_{13}, indicating that the isatin ring will probably be the favorite site for nucleophilic attacks.

The results also show that O_{13} atom is suitable site to undergo both nucleophilic and electrophilic attacks, probably allowing them to adsorb easily and strongly on the mild steel surface.

Table 6. Calculated Mulliken atomic charges and Fukui functions for the studied inhibitor calculated at B3LYP/6-31G(d,p) in gas, G and aqueous, A phases

Atom k	phase	q(N)	q(N+1)	q(N-1)	f_k^+	f_k^-	f_k^0
C_3	G	0,0022	0,1880	-0,0215	0,1858	0,0238	0,1048
	A	0,0977	0,2355	0,0303	0,1378	0,0674	0,1026
C_6	G	0,0516	0,2015	0,0116	0,1499	0,0400	0,0950
	A	0,1387	0,2213	0,0133	0,0827	0,1254	0,1040
Cl_{12}	G	-0,0086	0,2928	-0,0639	0,3014	0,0553	0,1784
	A	0,0547	0,2330	-0,0326	0,1783	0,0873	0,1328
O_{13}	G	-0,4680	-0,2722	-0,5312	0,1958	0,0632	0,1295
	A	-0,4576	-0,3385	-0,5871	0,1191	0,1294	0,1243

The final optimized geometries of E1 in gas (G) and aqueous (A), selected valence bond angle and dihedral angles and bond lengths are given in Figure 7.
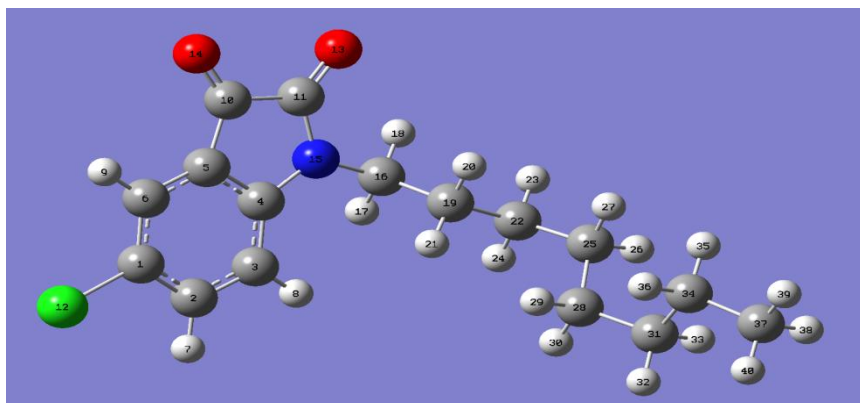
Figure 7. Optimized molecular structure calculated at B3LYP/6-31G(d, p) level of E1.

After the analysis of the theoretical results obtained, we can say that the molecule **E1** have a non-planar structure.


LUMO Gas   LUMO Aqueous

HOMO Gas   HOMO Aqueous
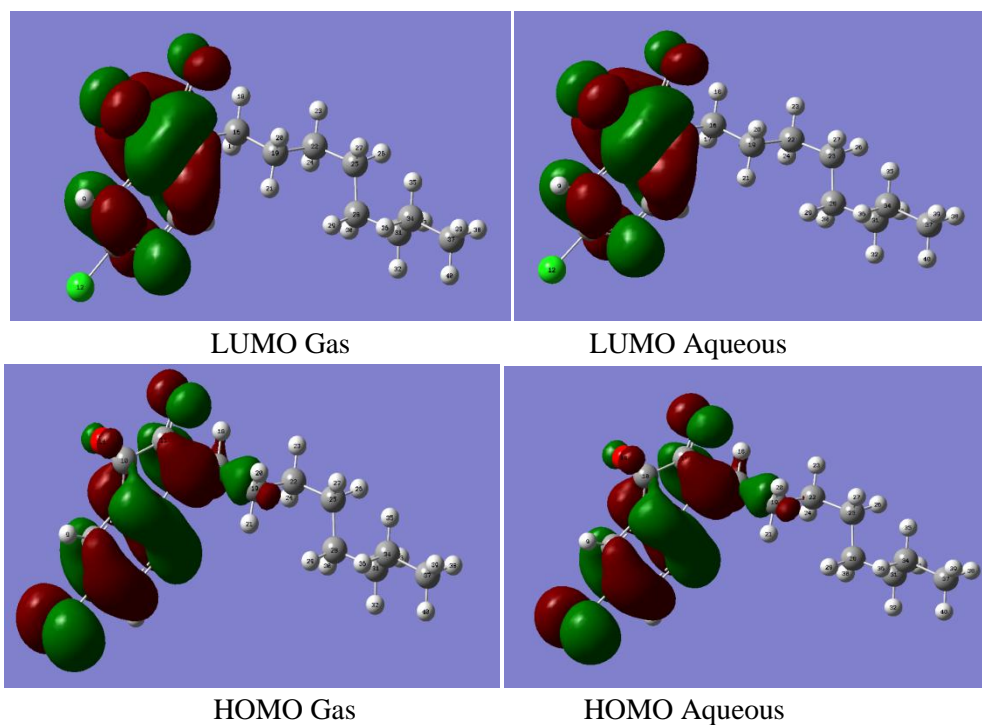
Figure 8: The HOMO and the LUMO electrons density distributions of the studied inhibitors computed at B3LYP/6-31G (d,p) level in gas and aqueous phases.

The inhibition efficiency afforded by the isatin derivative E1 may be attributed to the presence of electron rich Oxygen.

3.6. SEM studies

SEM micrographs of the mild steel surface after 6 h immersion at 308K in 1 M HCl in the absence and presence of 10^{-3}M of the inhibitor E1 are displayed in Figure 9. As evident from Figure 9, the mild steel surface is strongly attacked in the absence of inhibitor E1 due to the intensive metal dissolution, leading to highly porous surface with large and deep holes. In contrast, in the presence of the 5-chloro-1-octylindoline-2,3-dione (E1), the appearance of the steel surface is significantly improved, with almost no pores except for the polishing lines, that are observed on the micrograph. The observation of polishing lines in the presence of 5-chloro-1-octylindoline-2,3-dione (E1) (Figure 9) indicates their higher inhibition performances.
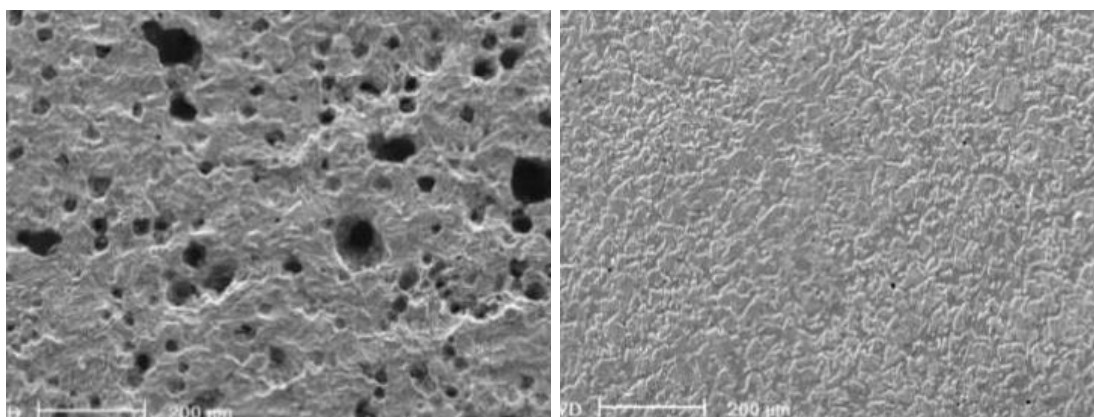
Figure 9. SEM micrographs of the mild steel surface after 6 h immersion at 308K in 1 M HCl: (a) without inhibitor; (b) containing 10^{-3}M E1.

Conclusion

The inhibition efficiency of mild steel corrosion in 1 M HCl by 5-chloro-1-octylindoline-2,3-dione (E1) has been investigated using gravimetric electrochemical measurement and quantum chemical calculations at (DFT/B3LYP/6-31G (d, p)) level of theory. The following conclusions were drawn from this study:

1. Reasonably good agreement was observed between gravimetric, potentiodynamic polarization and electrochemical impedance spectroscopy techniques.
2. E1 acts as a novel good inhibitor for the corrosion of mild steel in 1 M HCl. Inhibition efficiency values increase with the inhibitor concentration. The adsorption of E1 obeys Langmuir adsorption isotherm.
3. E1 is a mixed-type inhibitor in 1 M HCl, and the inhibition action is caused by geometric blocking effect. EIS spectra exhibit large capacitive loop at high frequencies. The addition of E1 to 1 M HCl solutions enhances Rct values while reduces Cdl values.
4. The calculated quantum chemical parameters such as HOMO-LUMO gap, EHOMO, ELUMO, dipole moment (μ) and total energy (TE) were found to give reasonably good correlation with the efficiency of the corrosion inhibition.

References

1. Hassan H.H., Abdelghani E., Amin M.A., *Electrochimica Acta*. 52 (2007) 6359
2. Hillis D., *Annals of the Rheumatic Diseases*. 69 (2014) 2131
3. Fouda A.S., Ellithy A.S., *Corros. Sci.* 51 (2009) 868.
4. Bahrami M.J., Hosseini S.M.A., Pilvar, P., *Corros. Sci.* 52 (2010) 2793.
5. Deng S., Li X., Fu H., *Corros. Sci.* 53 (2011) 822.
6. Solmaza R., Altunbas E., Kardas G., *Mater. Chem. Phys.* 125 (2011) 796.
7. Shi X., Suo T.A Z., LiuY., Avci R., *Surface & Coatings Technology*. 16 (2016) 9874.
8. Elayyachi M., Hammouti B., El Idrissi A., *Appl. Surf. Sci*. 249 (2005) 176.
9. Elayyachi M., El Idrissi A., Hammouti B., *Corros. Sci*. 48 (2006) 2470.
10. Pandeya S.N., Sriram D., Nath G., E. *Pharm. Acta Helv*. 74 (1999) 11
11. Sarangapani M., Reddy V.M., *Indian J. Pharm. Sci*. 56 (1994) 174.
12. Popp F.D., Parson R., Donigan B.E., *J. Heterocycl. Chem*. 17(1980) 1329.
13. Pandeya S.N., Sriram D., De Clercq E., Nath G. *Eur. J. Pharm. Sci*. 9 (1999) 25.
14. Singh G.S., Singh T., Lakhan R. *Indian J. Chem*. 36B (1997), 951.
15. Bhattacharya S.K., Chakrabarti S., *Indian J. Exp. Biol*. 36 (1998) 118.
16. Tribak Z., Kharbach Y., Haoudi A., Skalli M.K., Kandri Rodi Y., El Azzouzi M., Aouniti A., Hammouti B., Senhaji O., *J. Mater. Environ. Sci.* 7 (2016) 2006.
17. Frisch M.J., Trucks G.W., Schlegeletal H.B.., *Gaussian 09, Revision A.1, Gaussian, Inc., Wallingford, Conn, USA,* (2009).

18. Elmsellem H., Youssouf M. H., Aouniti A., Ben Hadd T., Chetouani A., Hammouti B. *Russian, Journal of Applied Chemistry*, 87 (2014) 744−753

19. Li J., Li H., Jakobsson M., Li S., Sjodin P., Lascoux M., *Mol. Ecol.* 21(1), (2012) 28-44.

20. Hjouji M.Y., Djedid M., Elmsellem H., Kandri Rodi Y., Benalia M., Steli H., Ouzidan Y., Ouazzani Chahdi F., Essassi E.M., and Hammouti B. *Der Pharma Chemica*. 8 (2016)85-95.

21. Elmsellem H., Harit T., Aouniti A., Malek F., Riahi A., Chetouani A., and Hammouti B., *Protection of Metals and Physical Chemistry of Surfaces*. 51 (2015) 873–884.

22. Efil K., Bekdemir Y. *Canadian Chemical Transactions*. 3 (2015) 85.

23. Pauling L., The nature of the chemical bond, 3rd edn. (Cornell University Press, Ithaca,) (1960).

24. Sen K.D.; Jorgenson, C. K. Eds. Structure and Bonding, Electronegativity; Springer: Berlin, 66 (1987).

25. Sen K.D., Mingos, D. M. P. (eds.), in Chemical Hardness, Structure and Bonding, Springer-Verlag,Berlin, 80 (1993) 11–25.

26. Parr R.G., Yang W., Density-Functional Theory of Atoms and Molecules. Oxford University Press, New York, (1989).

27. Geerlings P., de Proft F., Langenaeker W., Chem. Rev. 103 (2003) 1793.

28. Chermette H., *J. Comput. Chem*. 20 (1999)129.

29. Roy R.K., Pal S., Hirao K., *J. Chem. Phys*. 110 (1999) 8236.

30. Pearson R.G*., Inorg. Chem*., 27 (1988) 734.

31. Sastri, V.S. and Perumareddi, J.R., *Corrosion.* 3 (1997) 671.

32. Udhayakala P., Rajendiran T. V., Gunasekaran S., *Journal of Chemical, Biological and Physical Sciences* A, 2(3) (2012) 1151–1165.

33. Bentiss F., Lagrenee M., Traisnel M., Hornez J.C., *Corros. Sci*. 41(1999) 789.

34. Essaghouani A. L., Elmsellem H., Ellouz M., El Hafi M., Boulhaoua M., Sebbar N. K., Essassi E. M., Bouabdellaoui M., Aouniti A. and Hammouti B., *Der Pharma Chemica*. 8(2) (2016)297-305.

35. Ellouz M., Elmsellem H., Sebbar N. K., Steli H., Al Mamari K., Nadeem A., Ouzidan Y., Essassi E. M., Abdel-Rahaman I., Hristov P., *J. Mater. Environ. Sci*. 7(7) (2016)2482-2497.

36. Elmsellem H., Bendaha H., Aouniti A., Chetouani A., Mimouni M., Bouyanzer A., *Mor. J. Chem*. 2 (2014)1-9.

37. Elmsellem H., Elyoussfi A., Sebbar N. K., Dafali A., Cherrak K., Steli H., Essassi E. M., Aouniti A. and Hammouti B., *Maghr. J. Pure & Appl. Sci*. 1 (2015)1-10.

38. Elmsellem H., Karrouchi K., Aouniti A., Hammouti B., Radi S., Taoufik J., Ansar M., Dahmani M., Steli H., El Mahi B., *Der Pharma Chemica*, 7 (2015)237-245.

39. Elmsellem H., Elyoussfi A., Steli H., Sebbar N. K., Essassi E. M., Dahmani M., El Ouadi Y., Aouniti A., El Mahi B., Hammouti B., *Der Pharma Chemica*. 8(1) (2016) 248.

40. Elmsellem H., Basbas N., Chetouani A., Aouniti A., Radi S., Messali M., Hammouti B., *Portugaliae Electrochimica. Acta*, 2 (2014) 77.

41. Elmsellem H., Nacer H., Halaimia F., Aouniti A., Lakehal I., Chetouani A., Al-Deyab S. S., Warad I., Touzani R., Hammouti B, *Int. J. Electrochem. Sci*. 9 (2014) 5328.

42. Elmsellem H., Aouniti A., Youssoufi M.H., Bendaha H., Ben hadda T., Chetouani A., Warad I., Hammouti B., *Phys. Chem. News*, 70 (2013) 84.

43. Fouda A.S., Shalabi S.K., Elewady G.Y., Merayyed H.F., *Int. J. Electrochem. Sci*. 9 (2014) 7038–7058.

44. Elmsellem H., Aouniti A., Toubi Y., Steli H., Elazzouzi M., Radi S., Elmahi B., El Ouadi Y., Chetouani A., Hammouti B., *Der Pharma Chemica*. 7 (2015) 353-364.

45. Elmsellem H., Aouniti A., Khoutoul M., Chetouani A., Hammouti B., Benchat N., Touzani R., Elazzouzi M., *J. Chem. Pharm. Res*. 6 (2014)1216.

46. Al Mamari K., Elmsellem H., Sebbar N. K., Elyoussfi A., Steli H., Ellouz M., Ouzidan Y., Nadeem A., Essassi E. M., El-Hajjaji F., *J. Mater. Environ. Sci*. 7 (9) (2016) 3286-3299

47. Sikine M., Kandri Rodi Y., Elmsellem H., Krim O., Steli H., Ouzidan Y., Kandri Rodi A., Ouazzani Chahdi F., Sebbar N. K., Essassi E. M., *J. Mater. Environ. Sci*. 7 (4) (2016) 1386-1395.

48. Hjouji M.Y., Djedid M., Elmsellem H., Kandri Rodi Y., Ouzidan Y., Ouazzani Chahdi F., Sebbar N. K., Essassi E. M., Abdel-Rahman I., Hammouti B., *J. Mater. Environ. Sci.* 7 (4) (2016) 1425-1435

49. Lukovits I., Kalman E., Zucchi F., *Corrosion*. 57 (2001) 3-7.

50. Y. Filali Baba, H. Elmsellem, Y. Kandri Rodi, H. Steli, C. AD, Y. Ouzidan, F. Ouazzani Chahdi, N. K. Sebbar, E. M. Essassi, and B. Hammouti. *Der Pharma Chemica*. 8(4) (2016) 159-169.

(2017) ; http://www.jmaterenvironsci.com